Microbiology (2001), **147**, 561–570 Printed in Great Britain

NAD(P)H:menadione oxidoreductase of the amitochondriate eukaryote *Giardia lamblia*: a simpler homologue of the vertebrate enzyme

Lidya B. Sánchez,[1] Heidi Elmendorf,[2]† Theodore E. Nash[2] and Miklós Müller[1]

Author for correspondence: Lidya B. Sánchez. Tel: +1 212 327 8144. Fax: +1 212 327 7974. e-mail: sanchel@rockvax.rockefeller.edu

[1] Laboratory of Biochemical Parasitology, The Rockefeller University, 1230 York Avenue, New York, NY 10021, USA

[2] Laboratory of Parasitic Diseases, National Institute of Allergy and Infectious Diseases, National Institutes of Health, Bethesda, MD 20892, USA

The amitochondriate eukaryote *Giardia lamblia* contains an NAD(P)H:menadione oxidoreductase (EC 1.6.99.2) (glQR) that catalyses the two-electron transfer oxidation of NAD(P)H with a quinone as acceptor. The gene encoding this protein in *G. lamblia* was expressed in *Escherichia coli*. The purified recombinant protein had an NAD(P)H oxidoreductase activity, with NADPH being a more efficient electron donor than NADH. Menadione, naphthoquinone and several artificial electron acceptors served as substrate for the enzyme. glQR shows high amino acid similarity to its homologues in vertebrates and also to a series of hypothetical proteins from bacteria. Although glQR is considerably smaller than the mammalian enzymes, three-dimensional modelling shows similar arrangement of the secondary structural elements. Most amino acid residues of the mammalian enzymes that participate in substrate binding or catalysis are conserved. Conservation of these features and the similarity in substrate specificity and in susceptibility to inhibitors establish glQR as an authentic member of this protein family.

Keywords: menadione oxidoreductase, *Giardia lamblia*, DT-diaphorase

INTRODUCTION

NAD(P)H:menadione oxidoreductase, also called DT-diaphorase [NAD(P)H:quinone-acceptor oxidoreductase type 1; EC 1.6.99.2] (QR1), catalyses the two-electron reduction of quinones, quinone compounds and a variety of oxidants with NADPH or NADH as electron donors (Cui *et al*., 1995; Segura-Aguilar *et al*., 1992; Tedeschi *et al*., 1995). It is widely distributed in animals. The cytosolic enzymes from rat, mouse and human have been extensively studied and their crystal structure determined at high resolution (Faig *et al*., 2000; Li *et al*., 1995). QR1 is a homodimer of 273 amino acid subunits that binds two molecules of FAD and folds into five central parallel β-strands flanked on each side by connecting helices. The reaction mechanism as well as the residues interacting with FAD and with the two substrates have been elucidated in great detail by structural and enzymic studies (Chen *et al*., 1994; Cui *et al*., 1995; Faig *et al*., 2000; Foster *et al*., 2000; Li *et al*., 1995; Tedeschi *et al*., 1995). Another well-characterized homologue found in tissues is QR2 (Faig *et al*., 2000; Wu *et al*., 1997). This 230 amino acid protein is 49% identical to QR1, uses only non-phosphorylated nicotinamide derivatives such as *N*-ribosyl and *N*-alkyl dihydronicotinamide, and is not affected by characteristic QR1 inhibitors (Foster *et al*., 2000; Wu *et al*., 1997). The high-resolution crystal structure of QR2 (Foster *et al*., 1999) showed an overall structure very similar to that of QR1 but lacking its 47 amino acid C-terminal domain.

In spite of over 60 years of intensive studies neither the natural substrates nor the biological role of QR1 are completely elucidated. This enzyme has been implicated in the metabolism of vitamin K, maintenance of the reduced form of coenzyme Q in membranes, and detoxification of quinones and diverse anti-cancer

†**Present address:** Biology Department, Georgetown University, Washington, DC 20057, USA.

Abbreviations: QR, NAD(P)H:menadione oxidoreductase; QR1, QR type 1; rQR1, QR1 from rat; hQR1, QR1 from human; hQR2, QR type 2 from human; glQR1, *G. lamblia* QR1; DCIP, 2,6-dichorophenolindophenol; K_m^{app}, apparent Michaelis constant; MT, methyl red; MTT, 3-(4,5-dimethylthiazol-2-yl)-2,5-diphenyltetrazolium bromide; SOD, superoxide dismutase.

The GenBank accession number for the glQR1-encoding sequence reported in this paper is AF321405.

agents (Chen *et al*., 2000; Dinkova-Kostova & Talalay, 2000). Several oxidoreductases can reduce quinone compounds in the presence of NADH and NADPH via a one-electron transfer reaction, to a semiquinone, which in turn can reduce oxygen to form superoxides. In contrast, QR1 can reduce a variety of quinone compounds through a two-electron transfer reaction in the presence of NAD(P)H. The ability to participate in the reduction of several compounds by two-electron reduction processes prevents a one-electron redox cycling that generates reactive and toxic oxygen species and suggests a possible role of the DT-diaphorase as part of a cellular antioxidant defence system (Dinkova-Kostova & Talalay, 2000; Nakamura & Hayashi, 1994; Siegel & Ross, 2000; Tedeschi *et al*., 1995).

The distribution of these cytosolic enzymes in the living world remains essentially unknown. Interestingly, activity of a possibly closely related enzyme has been reported from two unrelated parasitic unicellular eukaryotes, the diplomonad *Giardia lamblia* (Weinbach *et al*., 1980) and the amoeba *Entamoeba histolytica* (Weinbach *et al*., 1977). Both species lack typical mitochondria and have a fermentative metabolism (Adam, 1991; Brown *et al*., 1998; Martinez-Palomo, 1982; Müller, 1998). They also have the ability to take up oxygen (Brown *et al*., 1998; Paget *et al*., 1989; Weinbach *et al*., 1980). The respiration is not linked to mitochondrial-type cytochrome oxidase and is not accompanied by oxidative phosphorylation. These organisms are exposed to varying levels of oxygen in their environment. It is likely that toxic oxygen derivatives are generated intracellularly and also in the gut tissues with which they are in contact. Their means to deal with the potential threat of oxidative stress are little known. Both species lack catalase, glutathione and glutathione reductase; moreover no superoxide dismutase (SOD) has been detected in *G. lamblia* (Brown *et al*., 1995). Proposed components of alternative mechanisms of oxygen detoxification (oxidation defence) in *G. lamblia* include a cytosolic H_2O-forming NADH oxidase, proposed to function as a terminal oxidase that removes excess reducing equivalents and as a component of the electron-transport pathway that protects oxygen-labile proteins by maintaining a reduced intracellular environment (Brown *et al*., 1995, 1996a, 1998); a membrane-associated NADH peroxidase associated with the observed H_2O_2 removal by viable trophozoites (Brown *et al*., 1995); and a thioredoxin-like disulfide reductase with a role in disulfide redox management (Brown *et al*., 1996b, 1998).

Although diverse electron-transport pathways have been proposed, the mechanisms and the redox components involved have not been elucidated completely. Quinones have been detected in both species and their involvement in respiration has been suggested (Ellis *et al*., 1994). Early studies showed that NADH and NADPH stimulated respiration, an observation that was interpreted as evidence for the presence of an active 'DT-diaphorase', NAD(P)H:quinone-acceptor oxidoreductase (EC 1.6.99.2) (Paget *et al*., 1989; Weinbach *et al*., 1977, 1980). Evidence for the presence of QR1 was provided by the increased NADPH oxidation in the presence of 1 mM menadione by a cytosolic fraction and its inhibition by 200 μM dicoumarol (Weinbach *et al*., 1980). Our identification and subsequent sequencing of a QR gene from *G. lamblia* enabled us to express this protein in *Escherichia coli*. Here we describe the properties of this enzyme and show that it is smaller than its mammalian homologues but is highly similar in its biochemical properties. Three-dimensional protein modelling revealed a basically similar folding but indicated certain differences in the interaction of the protein with FAD and its substrates.

METHODS

Organism and cell extracts. *G. lamblia* trophozoites (strain WB, provided by Dr Stephen Aley, University of Texas, El Paso, TX, USA) were cultured axenically at 37 °C in TYI medium (Keister, 1983). Exponential-phase trophozoites were harvested by chilling on ice for 10 min and centrifugation at 700 ***g*** at 4 °C for 7 min. The pellet was washed with phosphate-buffered saline, resuspended in 250 mM sucrose, 50 mM phosphate buffer pH 7·5 and 10 μg leupeptin ml^{-1}, and sonicated with five 30 s pulses with a Branson sonifier at 20 % duty cycle and output setting 2. After centrifugation at 100000 ***g*** for 1 h at 4 °C, the supernatant fraction was stored at −20 °C or used immediately.

Enzyme activity assays. The NAD(P)H-dependent reduction of menadione was monitored in a coupled assay, under aerobic conditions. Reduced menadione, menadiol, in turn reduces cytochrome, the absorbance of which can be followed at 550 nm ($\varepsilon_{550} = 29{\cdot}5\ mM^{-1}\ cm^{-1}$). Measurements were made in 50 mM Tris/HCl pH 7·5, 200 μM NADPH (as electron donor), 1 μM menadione (as electron acceptor) and 30 μM cytochrome *c*.

For other electron acceptors tested, the standard mixture contained 400 μM NADPH, 50 mM Tris/HCl pH 7·5 and one of the following: 0·15 mM 2,6-dichorophenolindophenol (DCIP), 1 mM potassium ferricyanide, 0·5 mM 3-(4,5-dimethylthiazol-2-yl)-2,5-diphenyltetrazolium bromide (MTT) or 50 μM methyl red (MT). The reactions were initiated by addition of the enzyme and the reduction of the acceptor was followed spectrophotometrically at 600 nm for DCIP ($\varepsilon = 21{\cdot}5\ mM^{-1}\ cm^{-1}$), 410 nm for potassium ferricyanide ($\varepsilon = 1\ mM^{-1}\ cm^{-1}$), 610 nm for MTT ($\varepsilon = 11{\cdot}3\ mM^{-1}\ cm^{-1}$) and 436 nm for MT ($\varepsilon = 18\ mM^{-1}\ cm^{-1}$). One unit of enzyme activity was defined as 1 μmol product formed per min per mg protein. All determinations were done at least in triplicate; means are shown ± SD where appropriate.

Molecular cloning. A gene encoding a putative NADPH:quinone oxidoreductase from *G. lamblia* was serendipitously isolated during the study of microtubule-associated genes. Based on the available sequence, the entire glQR1 coding region was amplified by PCR utilizing *G. lamblia* genomic DNA as template and the oligonucleotides glQR1-4F (sense: 5′-GACGACGACAAGGGATCCACATCGTCCTCTATTACTCC-3′) and glQR1-5R (antisense: 5′- GGACACAGACCCGGGTTACTCGAAGAGCTTCAGGTAGCT-3′). The sense primer introduced a *Bam*HI site immediately upstream of the ATG codon and the antisense primer a *Sma*I site downstream of the stop codon of the gene (sites underlined). The resulting 500 bp product, containing the full-length glQR1 coding region, was inserted into pCR2.1 vector

using a TA Cloning Kit (Invitrogen). Clones containing the glQR1 insert were verified by PCR and digested with *Bam*HI and *Sma*I to release the glQR1-coding insert, which was subsequently gel-purified and subcloned into plasmid pQE-32 (Qiagen). The glQR1 gene was placed in-frame with a histidine stretch encoded by the plasmid and under the control of an IPTG-inducible *lac* promoter. The nucleotide sequence of this construct was verified by primer walking and dye-primer terminator chemistries and assembled with the Seqman program of the Lasergene package (DNASTAR).

Expression and purification of the recombinant protein. *E. coli* M15(pREP4) containing the recombinant plasmid was grown at 37 °C in LB medium containing 100 μg ampicillin ml^{-1}, until an OD_{600} of 0·6 was reached. Subsequently 1 mM IPTG was added and incubation continued for an additional 6 h at 37 °C. Purification of the recombinant protein was performed using Ni-NTA resin following the manufacturer's (Qiagen) recommendations for purification of native cytoplasmic proteins.

Sequence analysis and protein modelling. Protein database searches were performed on the server of the National Center for Biotechnology Information by using the BLAST network service (Altschul *et al.*, 1997). The deduced amino acid sequence was aligned with the related sequences and the alignment was edited manually with the ED program of the MUST package (Philippe, 1993). Crystallographic coordinates for the DT-diaphorase QR1 of rat (file 1QRD), human (files 1D4A and 1DXO) and mouse (file 1DXQ), and the human QR2 (files 1QR2 and 2QR2), were obtained from the Protein Database. These were used as reference structures to calculate three-dimensional models of glQR1 using comparative protein modelling by satisfying spatial restraints as implemented in the program MODELLER V.4 (Šali & Blundell, 1998; Sánchez & Šali, 1997). The input to MODELLER was a multiple alignment of glQR1 with QRs of known structure. The resulting models of glQR1 without and with bound cofactor were subsequently evaluated using PROCHECK (Laskowski *et al.*, 1993) and the HOMOLOGY module from the package InsightII (Molecular Stimulation Inc.).

RESULTS

A 495 bp DNA fragment encompassing the full-length coding region of a putative NAD(P)H:quinone oxidoreductase of *G. lamblia* was inserted downstream of the promoter region of pQE-32 vector and expressed in *E. coli*. SDS-polyacrylamide gels and enzymic activity determination showed an active histidine-tagged recombinant glQR1 protein that was expressed in IPTG-induced cells containing the plasmid construct, but not in control cells transformed with the plasmid without insert or in uninduced cells. The molecular mass of the recombinant protein was 19 kDa, corresponding to that inferred from the nucleotide sequence. The presence of the protein band in the gel correlated with the presence of QR activity (data not shown) and an intensely yellow colour. The protein was purified and separated from endogenous bacterial proteins by affinity chromatography in Ni-NTA agarose and the purified preparation used for its biochemical characterization.

Catalytic properties

The purified recombinant protein reduced menadione and naphthoquinone with either NADPH (with a specific activity of 93·53 ± 6·56 and 88·87 ± 0·96 μmol min^{-1} mg^{-1}, respectively) or NADH (24·15 ± 2·39 and 18·28 ± 1·46 μmol min^{-1} mg^{-1}, respectively) as reductant. No activity was observed with 2-hydroxy-1,4-naphthoquinone-1,4-benzoquinone (BQ) and certain benzoquinone derivatives such as methyl-BQ, 2,6-dimethyl-BQ and 2,3-dimethoxy-5-methyl-BQ (data not shown).

Linear double-reciprocal plots were obtained by varying the concentration of menadione or naphthoquinone at constant concentrations of NADPH or NADH and vice versa. glQR1 had a similar and very high affinity for both menadione and naphthoquinone in the presence of either NADPH or NADH. K_m^{app} and k_{cat} values for both electron acceptors were within the same order of magnitude (Table 1). The enzyme was more efficient with menadione than with naphthoquinone, with either NADPH (2·2-fold) or NADH (1·8-fold) as the electron donor. With respect to the electron donor, glQR1 had similar affinities for NADPH and NADH in the presence of naphthoquinone and the reaction was similarly

Table 1. Kinetic parameters of glQR for the electron acceptors

NAD(P):menadione oxidoreductase activity was determined spectrophotometrically by measuring the reduction of cytochrome *c* at 550 nm. Each value is the mean of three to five sets of experiments ± SD. Kinetic parameters were determined from Lineweaver–Burk plots generated by using 5–50 μM menadione or naphthoquinone as the electron acceptor. K_i values were determined by varying the menadione or naphthoquinone concentration (5–20 μM) at several fixed concentrations of dicoumarol (0, 0·5, 1, 2, 5 and 10 μM).

Electron donor	Electron acceptor	K_m^{app} (μM)	k_{cat} (s^{-1})	k_{cat}/K_m (μM^{-1} s^{-1})	K_i (μM)
NADPH	Menadione	0·240 ± 0·030	34·83 ± 6·13	145·12	4·12 ± 0·60
	Naphthoquinone	0·59 ± 0·001	39·29 ± 0·68	66·59	5·11 ± 0·91
NADH	Menadione	0·188 ± 0·016	23·07 ± 0·59	121·39	0·95 ± 0·08
	Naphthoquinone	0·437 ± 0·031	29·93 ± 1·78	68·03	1·09 ± 0·12

Table 2. Kinetic parameters of glQR for the electron donors

NAD(P) : menadione oxidoreductase activity was determined spectrophotometrically by measuring the reduction of cytochrome *c* at 550 nm. Each value is the mean of three to five sets of experiments ± SD. Kinetic parameters were determined from Lineweaver–Burk plots generated by using 5–400 μM NADPH or 5–1000 μM NADH as the electron donor. K_i values were determined by varying the NADPH or NADH concentration (5–400 μM) at several fixed concentrations of dicoumarol (0, 0·5, 1, 2, 5 and 10 μM).

Electron acceptor	Electron donor	K_m^{app} (μM)	k_{cat} (s^{-1})	k_{cat}/K_m (μM^{-1} s^{-1})	K_i (μM)
Menadione	NADPH	30·85 ± 4·70	52·68 ± 1·95	1·71	0·364 ± 0·092
	NADH	549·96 ± 14·50	31·72 ± 5·77	0·06	0·524 ± 0·066
Naphthoquinone	NADPH	33·43 ± 2·16	47·51 ± 3·28	1·42	0·789 ± 0·080
	NADH	44·91 ± 2·73	62·66 ± 5·06	1·40	0·719 ± 0·068

Table 3. Effect of several compounds on glQR1, for different electron acceptors with NAPDH as electron donor

NAD(P) : menadione oxidoreductase activity was determined spectrophotometrically by measuring the reduction of the electron acceptors ferricyanide, MTT, MT or DCIP, in the absence or presence of several compounds at the concentrations indicated. Reduction of cytochrome *c* was determined when the electron acceptor was menadione. All assays were performed at least in duplicate. Values in parentheses are the specific activities for each electron acceptor (μmol min^{-1} mg^{-1}) determined using the standard assay mixture, and defined as 100 %. ND, Not determined.

Addition	Concn	Relative activity (%) with:				
		Ferricyanide	MTT	MT	DCIP	Menadione
None		100 (1618)	100 (228)	100 (43)	100 (16)	100 (93)
Dicoumarol	2 μM	46	24	99	87	22
	10 μM	18	14	78	71	2
	20 μM	8	11	52	29	ND
	50 μM	2	9	41	ND	ND
SOD	16 U	105	ND	ND	ND	106
	32 U	96	ND	ND	ND	90–107
Catalase	200 U	109	ND	ND	ND	91
β-Mercaptoethanol	100 μM	145	96	56	100	60
DTT	100 μM	134	113	70	ND	52
N-Ethylmaleimide	50 μM	118	114	65	ND	76
	250 μM	45	90	38	ND	30
L-Cysteine	10 μM	145	99	79	ND	60
	50 μM	132	145	83	ND	9
1,10-Phenathroline	10 μM	32	117	78	37	27
	50 μM	24	44	66	40	9
Quercetin	10 μM	50	27	41	103	83
	50 μM	4	23	18	75	19
Quinacrine dihydrochloride	10 μM	16	77	39	ND	20
	50 μM	16	35	35		5

efficient (Table 2). In contrast, in the presence of menadione, glQR1 had a much higher affinity for NADPH (the K_m^{app} for NADPH was 18-fold lower than that for NADH) and the reaction was about 29-fold more efficient. With naphthoquinone as electron acceptor, glQR1 became highly specific for NADH. The

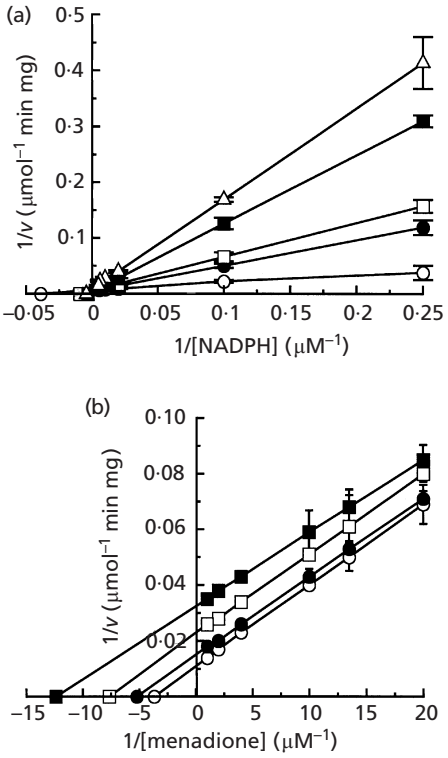

Fig. 1. (a) Competitive inhibition of glQR1 by dicoumarol with respect to the electron donor NADPH in the presence of menadione as acceptor. The concentrations of dicoumarol were 0 (○), 0·5 μM (●), 1 μM (□), 2 μM (■) and 3 μM (△). (b) Uncompetitive inhibition of glQR1 by dicoumarol with respect to the electron acceptor menadione in the presence of NADPH as donor. The concentrations of dicoumarol were 0 (○), 2 μM (●), 5 μM (□) and 7·5 μM (■). The data represent the mean (±SD where appropriate) of two to five determinations.

increase in catalytic efficiency for NADH, in the presence of naphthoquinone compared with menadione, resulted mainly from a much larger effect on the K_m^{app} for NADH (12·5-fold higher than that for NADPH), and to a lesser extent in the k_{cat} value (1·9-fold lower). glQR1 had a much higher affinity for menadione, with NADH as donor, than the human, rat and mouse enzymes ($K_m^{app} = 2{\cdot}7 \pm 0{\cdot}3$ μM, $2{\cdot}5 \pm 0{\cdot}1$ μM and $4{\cdot}3 \pm 0{\cdot}4$ μM, respectively), while its affinity for NADH was lower ($K_m^{app} = 220 \pm 10$ μM, 110 ± 10 μM and 210 ± 20 μM, respectively) (Chen *et al.*, 1999).

glQR1 was also able to reduce several alternative electron acceptors with NADPH (Table 3) or NADH (not shown) as electron donor. In the presence of NADPH, the reduction rates of the DCIP and MT (specific activities of $16{\cdot}11 \pm 1{\cdot}38$ μmol min^{-1} mg^{-1} and $43{\cdot}16 \pm 1{\cdot}92$ μmol min^{-1} mg^{-1}, respectively) were much lower than the reduction rate of menadione ($93{\cdot}53 \pm 6{\cdot}56$ μmol min^{-1} mg^{-1}), whereas they were higher for ferricyanide and MTT (specific activities of 1617 ± 44 μmol min^{-1} mg^{-1} and 288 ± 52 μmol min^{-1} mg^{-1}, respectively). NADPH was a more efficient electron donor, with reduction rates for ferricyanide and MTT about 3·3 and 4·8 times higher when compared to NADH as a donor (data not shown). Reduction of the different acceptors did not require an intermediate electron carrier: no significant changes in the rates of the process were observed upon addition of 1–5 μM menadione.

Inhibitors and enzyme effectors

The activity of recombinant glQR1 protein decreased by 22% in the presence of 1 μM dicoumarol, a strong inhibitor of the NADPH:quinone reductase reaction, and was essentially abolished at 10 μM. The susceptibility to dicoumarol suggested that glQR1 catalysed a diaphorase- or QR1-type oxidoreductase activity. Dicoumarol was a competitive inhibitor (Table 2) with respect to both NADPH (Fig. 1a) and NADH, with both menadione and naphthoquinone. On the other hand, uncompetitive inhibition was observed with menadione (Fig. 1b) and naphthoquinone (Table 1). Dicoumarol at 2 μM inhibited 54% and 76% of the ferricyanide and MTT reductase activities, while 20 μM was required for a comparable inhibition of the reduction of MT and DCIP (Table 3).

Several compounds tested modified the oxidoreductase activity for the several electron acceptors in a similar way (activation or inhibition) but to a different extent. FAD, FMN or pyridoxal phosphate (20–50 μM) did not affect the enzyme activity (not shown); however, the flavin antagonists quercetin and quinacrine dihydrochrloride (10–50 μM) were inhibitory. This suggests that glQR is a flavoenzyme, with the flavin tightly bound, since centrifugation of a protein fraction through a membrane to remove low-molecular-mass species (e.g. FAD/FMN) did not affect glQR1 activity. Catalase and SOD had no effect on the glQR activity.

Of the chelators tested, EDTA (100–250 μM) did not affect the reduction of the different acceptors but 1,10-phenanthroline was a strong inhibitor of the enzyme (Table 3). Reducing agents such as 2-ME, DTT and L-cysteine, and the alkylating reagent *N*-ethylmaleimide, inhibited the reduction of menadione and MT to some extent, while ferricyanide and MTT reduction were not affected or somewhat stimulated. Ferricyanide reduction required a higher *N*-ethylmaleimide concentration for inhibition. While cysteine inhibited menadione and MT reductase it enhanced ferricyanide and MTT reduction. Ouabain and chloroquine (10–50 μM) as well as the mitochondrial electron transport inhibitors KCN and NaN_3 (10–50 μM) had no effect on the glQR activity (data not shown).

QR1 activity in homogenates

G. lamblia homogenates supported the reduction of cytochrome, dependent on the concentration of NADPH, menadione and protein lysate, with a specific activity of 104–294 nmol min^{-1} mg^{-1}. Both menadione and naphthoquinone mediated cytochrome reduction irrespective of whether the hydrogen donor was

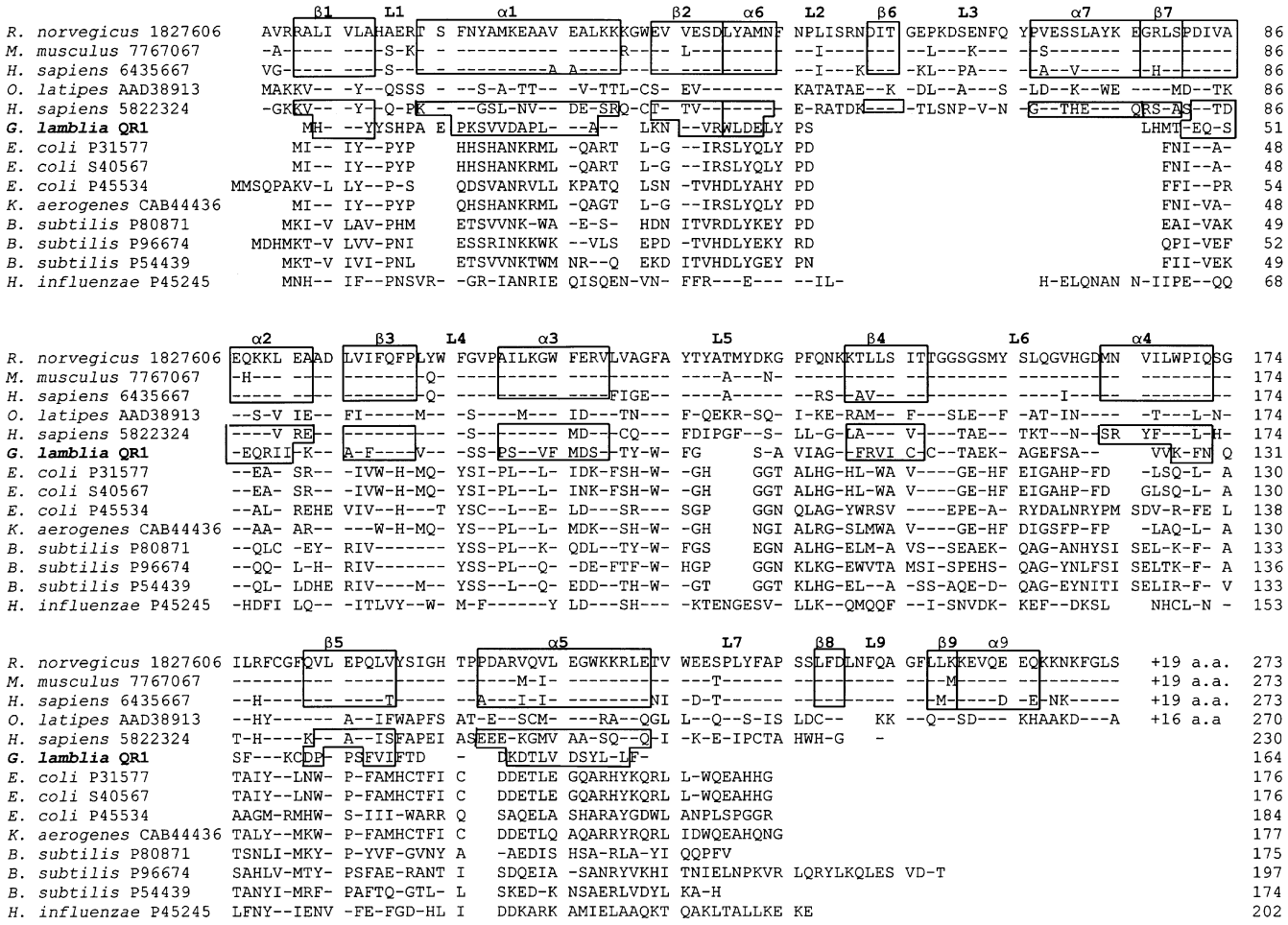

Fig. 2. Amino acid sequence alignment of the glQR1 sequence with several homologous genes from other organisms. Database accession numbers are indicated after the species name. The number of amino acids omitted at the C-terminus of the vertebrate sequences is indicated at the end of the sequences. Dashes represent residues identical to those of the rQR1 sequence; empty spaces represent positions with a gap. The numbering of the amino acid residues for each protein is indicated on the right. Predicted secondary structural elements of the glQR1 sequence and those of the vertebrate enzymes whose X-ray crystallographic structure is available are indicated above the sequence: sheets (β); helices (α) and loops (L). Sheets and helices are also highlighted by boxes. The numbering following the secondary structural elements corresponds to that for rQR1.

NADPH or NADH. Oxygen radical generation in the NADPH:menadione oxidoreductase reaction was investigated by examining the effect of catalase and SOD, which inhibit the superoxide ($O_2^{\cdot-}$)-mediated reduction of cytochrome *c*. No effect of catalase was observed, while the oxidoreductase activity of the homogenates decreased about 50% in the presence of SOD (data not shown). This indicated that a fraction of the NAD(P)H:quinone oxidoreductase activity generated $O_2^{\cdot-}$, possibly by the redox recycling of the menasemiquinone intermediate, which was responsible for cytochrome reduction, while another fraction was able to directly oxidize cytochrome *c*, without $O_2^{\cdot-}$ formation.

Dicoumarol (10 μM) inhibited NADP:menadione oxidoreductase activity by 22–24%, suggesting the presence in *G. lamblia* homogenates of oxidoreductases with different dicoumarol sensitivities. The partial effect of SOD and dicoumarol on the total activity of *G. lamblia* homogenates suggests that more than one enzymic activity is mediating the oxidation of NAD(P)H with the concomitant reduction of the quinone. However, the proportion of each one cannot be distinguished in the crude homogenates since more than one enzyme contributes to the reduction of the same electron acceptor.

Amino acid sequence

A BLAST search of the GenBank/SWISS-PROT non-redundant sequence database surprisingly gave only 14 significant ($P < 4e-05$) matches. These included sequences from mammals, a fish and a few eubacterial ORFs. No significant matches were found in the completely sequenced eukaryotic genomes of the yeast

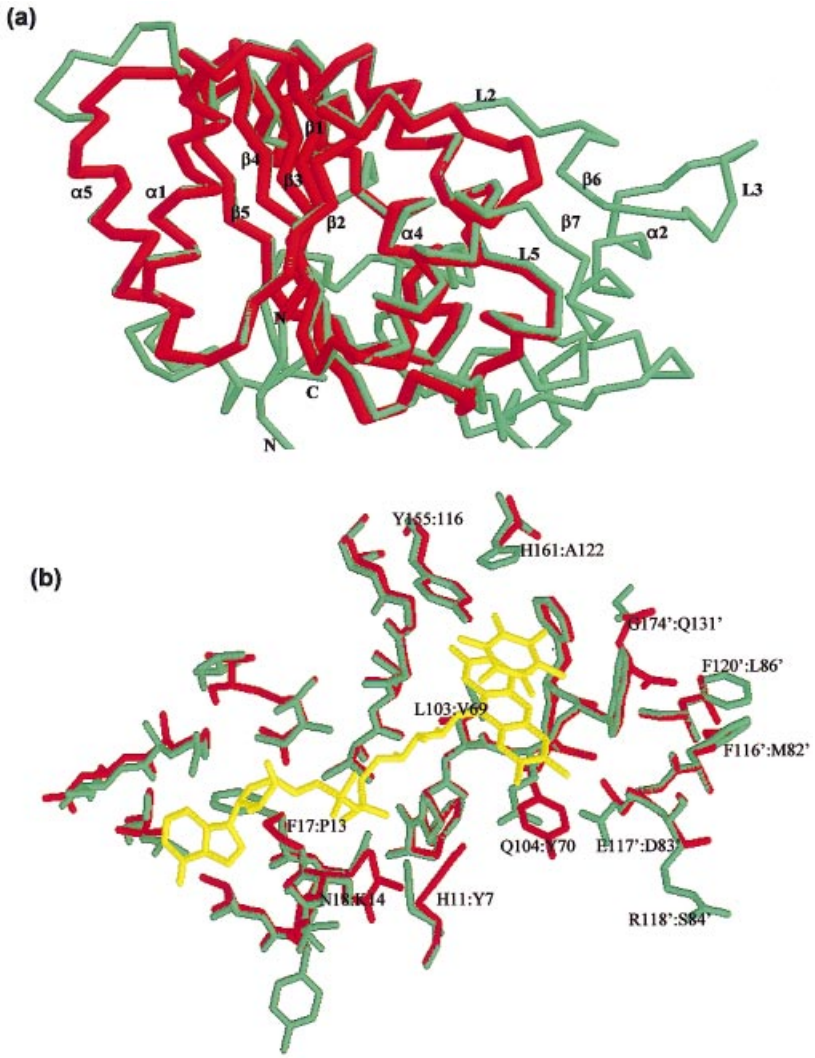

Fig. 3. (a) Superposition of the peptide chain from Cα-atoms of the glQR1 (red) and the hQR1 (green). Helices, sheets and loops are indicated by β, α and L, respectively, followed by a number according to the rQR1 sequence (Li *et al.*, 1995). (b) Superposition of residues involved in binding of the cofactor FAD and the quinone substrate (yellow) and those involved in catalysis for the glQR1 (red) and the hQR1 (green). Substituted amino acids are indicated by the rQR1 amino acid number followed by the glQR1 amino acid number.

Saccharomyces cerevisiae and in the protostome animals *Caenorhabditis elegans* and *Drosophila melanogaster*. The products of the eubacterial ORFs have not been characterized biochemically, but their high sequence similarity indicates analogous functions. The sequences belong to two separate size classes. Those from vertebrates were 273 amino acid residues long, with the exception of a human paralogue, QR2, of 230 residues, while the eubacterial ones, together with glQR, were significantly shorter. An amino acid alignment (Fig. 2) showed that the differences in lengths were accounted for primarily by an extended C-terminal end (61 amino acids longer) and a long insertion in the vertebrate sequences (Fig. 2), corresponding to residues 54–74 of QR1. There is a shorter insertion in the same region also in the *Haemophilus influenzae* ORF. glQR1 was overall rather divergent from all other sequences. While it was easily aligned with the rest in the C-terminal part of the sequence (from residue 43), the alignment proposed for the first 42 residues was less unambiguous but was confirmed statistically.

A maximum-likelihood-based phylogenetic reconstruction (data not shown) separated the sequences into three groups, largely in accordance with their overall length, which were supported by high bootstrap values. Although glQR shares a common ancestor with the eubacterial group, it is positioned between that group and the vertebrate group. In view of its great divergence from all other sequences and the extremely limited number of species available, no clear conclusions can be made of its genuine phylogenetic affinities.

Three X-ray structures of QR1 and QR2 were used to develop three-dimensional models of glQR1 to gain insight into the structural features of the enzyme that might correlate with some of the observed affinity similarities/differences of cofactor and inhibitor binding. The lowest energy structures were selected for a more detailed analysis of the active site (amino acid residues within 6 Å [0·6 nm] of the cofactor or the substrate). The models generated satisfied the overall stereochemical criteria implemented in PROCHECK as well as the protein structure evaluation test of the program Verify 3D. Atomic distances and potential hydrogen bonds were calculated with the HOMOLOGY

module of InsightII. The secondary structural elements identified in glQR1 are denoted by numerals as described in rQR1 (Li *et al*., 1995). Numbering of the amino acid residues when referred to in the text corresponds to the rat QR1 (rQR1) and glQR1 as indicated in Fig. 2. Amino acid residues on the second chain, contacting the cofactor or substrates, are denoted by the amino acid number followed by a prime (′).

The glQR1 N-terminal segment (residues 1–36) consists of two β-sheets and an α-helix overlapping β1, L1, α1 (4 amino acids shorter in *G. lamblia*) and β2 of QR1 (residues 1–40). In glQR1, this segment is connected through a 12 amino acid loop (residues 35–46) to the central region, instead of the much larger stretch of QR1 (residues 41–76) comprising loops L2 and L3, helices α6 and α7 and the β-sheet β6. The central region in glQR1 (residues 47–85) overlaps α2, β3, L4 and α3 of QR1 (residues 81–119). A shorter loop region (residues 87–101) overlaps L5 of QR1 (residues 120–140) and connects the C-terminal portion containing β4, L6, α4 (3 amino acids shorter in *G. lamblia*), β5 and α5 of QR1 (residues 141–212). glQR1 lacks a region corresponding to the C-terminal region of QR1 encompassing loops L7 and L9, β-sheets β8 and β9 and helix α8.

Superposition of the glQR1 models on the crystallographic structures of QR1 (Fig. 3) and QR2 shows that both the overall protein fold (Fig. 3a) and the clefts contacting the isoalloxazine ring of the cofactor FAD and the donor/acceptor part of the substrates (the quinone and the nicotinamide moiety of NADPH) are highly conserved. In contrast, significant differences were found in the region of clefts contacting the adenosine ribose portion of NAD(P)H and the ribitol, the diphosphate and adenosine moieties of FAD, due not only to amino acid substitutions but also to deletion of some of the structural elements forming the clefts (Fig. 3b).

FAD binding. In the different models calculated for glQR1, amino acids anchoring the isoalloaxine moiety of FAD through hydrogen bonds include Y70, W71, F72, T108, G110, G111 and Y116, which are conserved and structurally overlap Y104, W105, F106, T147, G149, G150 and Y155 in QR1; Y70 overlaps Q104 in the mouse and human QR1 and V69 (of glQR1) overlaps L103 in QR1. On the other side of the isoalloxazine ring are found M82′, D83′, S84′ and L86′, whose α-carbon backbones superimpose those of F116′, E117′, R118′, F120′ of QR1, respectively, although their side chains are oriented out of the cleft.

There are differences in the region of the cleft accommodating the ribose, the diphosphate and the adenosine moieties of FAD. Amino acids interacting with this portion of the molecule FAD in QR1 include H11, F17, N18 and R200, which are substituted by Y7, P13, K14 and K150, respectively. The main chain of these residues is packed very closely to the cofactor but they seem not to be involved in any specific interactions; in glQR1 their side chains are shorter or shifted away from the FAD molecule, preventing direct contact with the cofactor. Amino acids interacting with FAD, I50, Y67, P68, E117, which are part of L2 and α7, are absent in glQR1.

Quinone binding. Amino acids contacting the quinone substrate include W105, F106 and F178′ (forming the internal wall of the pocket) and G1149, G150 (at the entrance of the pocket), which superimpose the W71, F72, F135′ G110 and G111 of QR1, respectively. Y126′, H161 and G174′ are substituted by F92′, A122 and Q131′, while P68′, Y128′ and H194 are missing.

NAD(P)H binding. More dramatic differences are found in the cleft that binds the adenosine moiety of NADPH, mainly due to the loss of protein–substrate contacts due to a truncation of loop L9 (which removes contacts mediated by L230, N231, F232 and F236) and a 5 amino acid deletion of loop 5 (which removes potential contacts of Y128′, A129′ and T130′, Y132). Close to the nicotinamide moiety with the potential to form hydrogen bonds or van der Waals contacts are M154 and on the second chain Y126′, and F178′, which are structurally overlapped by glQR1 K115, F92′ and F135′, respectively. Also within the pocket, the amino acid stretch TTGGS (residues 147–151 of the QR1 enzyme), suggested to be a part of the NADH-binding site (Li *et al*., 1995), is superimposed by TCGGT (residues 108–111 of glQR1). There are no residues overlapping Y128′ and H194.

Overall structure of the active site. In glQR1, the half of the active site that accommodates the isoalloxazine ring of FAD, the quinone and the nicotinamide part of NADPH and where the enzymic hydride transfer takes place is well conserved when compared with QR1. It provides most of the amino acids that interact with the cofactors and the substrate. Toward the other half of the active site, more dramatic differences are found; several contacts to the adenosine ribose part of the cofactors are not present, mainly due to deletions of the amino acids involved in these contacts. Amino acids or structural domains of QR1 with the potential to adopt different conformations facilitating the closing–opening of the active site and mediating different interactions with the substrates are not present in glQR1. The shielding (from water and possibly reactions with oxygen) provided mainly by the interactions between Y128′ and H161 and F232 (Faig *et al*., 2000) seems not to take place in glQR1 due to the absence of the first two amino acids and a substitution of the third by A122. On the other hand, in the region superposing Y128′ of QR1, the polypeptide chain of glQR1 (within the shorter loop L5) started bending around F92 (which overlaps Y126′ of QR1) away from the cofactor. Similar is the case of H194 within the shorter helix α5. Together with the absence of a residue overlapping P68′, the absence of H194 leaves a wider entrance to the active site in glQR1. Of the two amino acid residues proposed to directly participate in the charge relay that takes place in the obligatory two-electron transfer reaction, Y155 of QR1 is conserved in glQR1 and overlaps Y116. However, H161 of QR1 is

substituted in glQR1 by A122, which cannot function in the charge relay suggested. H161 participates in the catalytic reaction and in fact the k_{cat} for a mutant hH161Q is only 8% of the wild-type hQR1, but it does not interrupt the two-electron transfer reduction of menadione (Chen *et al*., 1999).

DISCUSSION

We have cloned and expressed a functional NADPH:menadione oxidoreductase of *G. lamblia*. Two lines of evidence support this conclusion. First, the amino acid sequence of the *G. lamblia* gene shows considerable homology to known QR genes from animal tissues. Second, a recombinant plasmid containing glQR1 and transfected into *E. coli* encoded a catalytically active QR, resembling the kinetic properties and inhibitor susceptibility characteristic of QR1s from other species. The most conserved region of glQR1 extends over the QR1 region containing several amino acid residues implicated in substrate and cofactor binding and catalysis, which suggests that both enzymes utilize similar catalytic mechanisms. The enzyme was susceptible to dicoumarol. Superoxide generation in the reaction was ruled out since glQR1 activity was not affected by SOD, suggesting a two-electron reduction of menadione.

glQR1 is a much shorter protein; however, biochemically it is an authentic QR. It contains most of the elements of secondary structure as QR1, defining a minimal structure capable of supporting QR activity. glQR1 lacks loop 9 and part of loop L5, which in QR1 undergo the largest structural changes upon binding of NAD(P)H. These differences and substitutions of amino acids located at the entrance of the active site define a wider cleft, which possibly lacks the adaptability to modulate the interactions with the cofactors/substrate that has been proposed for QR1. However, the broad spectrum of electron acceptors glQR1 can utilize shows that its active site can accommodate molecules of varying size and structure. From the crystal structures is clear that the C-terminal region of QR1 contributes to the binding of the pyrophosphate–ribose adenine moiety of the cofactor. However, the lack of the C-terminal domain in glQR1 (truncated at residue 212) and its ability to utilize NAD(P)H shows that these contacts seem not to discriminate electron donor specificity. This correlates with the fact that QR2, also lacking the C-terminal domain (truncated at residue 230) cannot utilize NAD(P)H as electron donors (Wu *et al*., 1997).

The substrate specificity and inhibitor susceptibility of glQR1 are similar to those seen in other characterized QR1s. Inhibition by flavoantagonists and the conservation of most of the residues involved in the contact of the flavin moiety suggest that the *G. lamblia* is also a flavoprotein. A role of flavoproteins in *G. lamblia* respiration has been suggested in initial experiments by the inhibitory effect of flavoantagonists on oxygen uptake and NADPH oxidation (Paget *et al*., 1989; Weinbach *et al*., 1980).

There is no experimental information on the physiological function of QR1. Since NAD(P)H is used as an electron donor one could speculate that the enzyme could be involved in nicotinamide metabolism or could link pyrimidine nucleotide oxidation to the reduction of a substrate to maintain the steady supply of oxidized pyrimidine nucleotides [NAD(P)H] for glycolysis. The *in vivo* substrates of glQR1 and its physiological role in *G. lamblia* metabolism have not been determined. glQR1 has the ability to utilize a variety of electron acceptors (as is also the case for the enzyme in other organisms) such as naphthoquinones and several artificial electron acceptors; thus it could remove as yet unidentified oxidants which otherwise would be reduced to a free-radical state or form an intermediate species that would rapidly react with nucleophiles (e.g. reduced thiol compounds such as cysteine, depleting the pools of reduced nucleophiles and nicotinamide). In general it could be part of a defensive network which protects cells against redox cycling oxidative stress and other toxic effects caused by exposure to quinones and other cellular oxidants.

Sequencing and characterization of the NAD(P)H: menadione oxidoreductase of the amitochondriate *G. lamblia* demonstrates the presence of this enzyme among eukaryotes outside of vertebrates. Although biochemical data suggest the existence of similar activities in other eukaryotes, the known taxonomic restrictedness of this enzyme is striking and needs an explanation. The sparse distribution could reflect divergence of homologues beyond the sensitivity of BLAST searches. If this consideration is valid, the significant sequence conservatism of the enzyme among a few eubacteria and eukaryotes as diverse as vertebrates and diplomonads is the more surprising and might bear the trace of horizontal gene transfers. The evolutionary history of this gene clearly deserves further studies.

ACKNOWLEDGEMENTS

We acknowledge the assistance and instruction by Dr András Fiser in three-dimensional-protein modelling. This study was supported by US Public Health Service Grant AI 11942.

REFERENCES

Adam, R. D. (1991). The biology of *Giardia* spp. *Microbiol Rev* **55**, 706–732.

Altschul, S. F., Madden, T. L., Schaffer, A. A., Zhang, J., Zhang, Z., Miller, W. & Lipman, D. J. (1997). Gapped BLAST and PSI-BLAST: a new generation of protein database search programs. *Nucleic Acids Res* **25**, 3389–3402.

Brown, D. M., Upcroft, J. A. & Upcroft, P. (1995). Free radical detoxification in *Giardia duodenalis*. *Mol Biochem Parasitol* **72**, 47–56.

Brown, D. M., Upcroft, J. A. & Upcroft, P. (1996a). A H_2O producing NADH oxidase from the protozoan parasite *Giardia duodenalis*. *Eur J Biochem* **241**, 155–161.

Brown, D. M., Upcroft, J. A. & Upcroft, P. (1996b). A thioredoxin reductase-class of disulphide reductase in the protozoan parasite *Giardia duodenalis*. *Mol Biochem Parasitol* **83**, 211–220.

Brown, D. M., Upcroft, J. A., Edwards, M. R. & Upcroft, P. (1998). Anaerobic bacterial metabolism in the ancient eukaryote *Giardia duodenalis*. *Int J Parasitol* **28**, 149–164.

Chen, S., Clarke, P. E., Martino, P. A., Deng, P. S. K., Yeh, C.-C., Lee, T. D., Prochaska, H. J. & Talalay, P. (1994). Mouse liver NAD(P)H:quinone acceptor oxidoreductase: protein sequence analysis by tandem mass spectrometry, cDNA cloning, expression in *Escherichia coli*, and enzyme activity analysis. *Protein Sci* **3**, 1296–1304.

Chen, S., Wu, K., Zhang, D., Sherman, M., Knox, R. & Yang, C. S. (1999). Molecular characterization of binding of substrates and inhibitors to DT-diaphorase: combined approach involving site-directed mutagenesis, inhibitor-binding analysis, and computer modeling. *Mol Pharmacol* **56**, 272–278.

Chen, S., Wu, K. & Knox, R. (2000). Structure–function studies of DT-diaphorase (NQO1) and NRH:quinone oxidoreductase (NQO2). *Free Radic Biol Med* **29**, 276–284.

Cui, K., Lu, A. Y. H. & Yang, C. S. (1995). Subunit functional studies of NAD(P)H:quinone oxidoreductase with a heterodimer approach. *Proc Natl Acad Sci U S A* **92**, 1043–1047.

Dinkova-Kostova, A. T. & Talalay, P. (2000). Persuasive evidence that quinone reductase type 1 (DT diaphorase) protects cells against the toxicity of electrophiles and reactive forms of oxygen. *Free Radic Biol Med* **29**, 231–240.

Ellis, J. E., Setchell, K. D. R. & Kaneshiro, E. S. (1994). Detection of ubiquinone in parasitic and free-living protozoa, including species devoid of mitochondria. *Mol Biochem Parasitol* **65**, 213–224.

Faig, M., Bianchet, M. A., Talalay, P., Chen, S., Winski, S., Ross, D. & Amzel, L. M. (2000). Structures of recombinant human and mouse NAD(P)H:quinone oxidoreductases: species comparison and structural changes with substrate binding and release. *Proc Natl Acad Sci U S A* **97**, 3177–3182.

Foster, C. E., Bianchet, M. A., Talalay, P., Zhao, Q. & Amzel, L. M. (1999). Crystal structure of human quinone reductase Type 2, a metalloflavoprotein. *Biochemistry* **38**, 9881–9886.

Foster, C. E., Bianchet, M. A., Talalay, P., Faig, M. & Amzel, L. M. (2000). Structures of mammalian cytosolic quinone reductases. *Free Radic Biol Med* **29**, 241–245.

Keister, D. (1983). Axenic culture of *Giardia lamblia* in TYI-S-33 medium supplemented with bile. *Trans R Soc Trop Med Hyg* **77**, 487–488.

Laskowski, R. A., McArthur, M. W., Moss, D. S. & Thornton, J. M. (1993). PROCHECK: a program to check the stereochemical quality of protein structures. *J Appl Cryst* **26**, 283–291.

Li, R., Bianchet, M. A., Talalay, P. & Amzel, L. M. (1995). The three-dimensional structure of NAD(P)H:quinone reductase, a flavoprotein involved in cancer chemoprotection and chemotherapy: mechanism of the two-electron reduction. *Proc Natl Acad Sci U S A* **92**, 8846–8859.

Martinez-Palomo, A. (1982). *The Biology of Entamoeba histolytica*. Chichester: Research Studies Press.

Müller, M. (1998). Enzymes and compartmentation of core energy metabolism of anaerobic protists – a special case in eukaryotic evolution? In *Evolutionary Relationships among Protozoa*, pp. 109–131. Edited by G. H. Coombs, K. Vickerman, M. A. Sleigh & A. Warren. Dordrecht: Kluwer.

Nakamura, M. & Hayashi, T. (1994). One- and two-electron reduction of quinones by rat liver subcellular fractions. *J Biochem* **115**, 1141–1147.

Paget, T. A., Jarroll, E. L., Manning, P., Lindmark, D. G. & Lloyd, D. (1989). Respiration in the cysts and trophozoites of *Giardia muris*. *J Gen Microbiol* **135**, 145–154.

Philippe, H. (1993). MUST, a computer package of Management Utilities for Sequences and Trees. *Nucleic Acids Res* **21**, 5264–5272.

Šali, A. & Blundell, T. L. (1998). Comparative protein modelling by satisfaction of spatial restraints. *J Mol Biol* **234**, 779–815.

Sánchez, R. & Šali, A. (1997). Evaluation of comparative protein structure modeling by Modeller-3. *Proteins Struct Funct Genet* **Suppl. 1**, 50–58.

Segura-Aguilar, J., Kaiser, R. & Lind, C. (1992). Separation and characterization of isoforms of DT-diaphorase from rat liver cytosol. *Biochim Biophys Acta* **1120**, 33–42.

Siegel, D. & Ross, D. (2000). Immunodetection of NAD(P):quinone oxidoreducatase 1 (NQO1) in human tissues. *Free Radic Biol Med* **29**, 246–253.

Tedeschi, G., Chen, S. & Massey, V. (1995). DT-diaphorase. Redox potential, steady-state, and rapid reaction studies. *J Biol Chem* **270**, 1198–1204.

Weinbach, E. C., Harlow, D. R., Claggett, C. E. & Diamond, L. S. (1977). *Entamoeba histolytica*: diaphorase activities. *Exp Parasitol* **41**, 186–197.

Weinbach, E. C., Claggett, C. E., Keister, D. B., Diamond, L. S. & Kon, H. (1980). Respiratory metabolism of *Giardia lamblia*. *J Parasitol* **66**, 347–350.

Wu, K., Knox, R., Sun, X. Z., Joseph, P., Jaiswal, A. K., Zhang, D., Deng, P. S. K. & Chen, S. (1997). Catalytic properties of NAD(P)H:quinone oxidoreductase-2 (NQO2). a dihydronicotinamide ribose dependent oxidoreductase. *Arch Biochem Biophys* **347**, 221–228.

Received 1 September 2000; revised 21 November 2000; accepted 1 December 2000.